

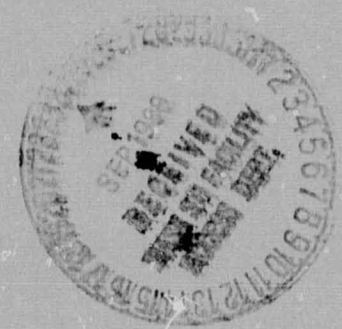


**Battelle**

Columbus Laboratories

(NASA-CR-161554) SSME TURBOPUMP BEARING N80-31794  
ANALYTICAL STUDY Final Report (Battelle  
Columbus Labs., Ohio.) 33 p HC A03/MF A01  
CSCS 131 Unclass  
G3/37 28594

# Report



FINAL REPORT

on

SSME TURBOPUMP BEARING ANALYTICAL STUDY

to

NATIONAL AERONAUTICS AND SPACE ADMINISTRATION  
GEORGE C. MARSHALL SPACE FLIGHT CENTER

by

J.W. Kannel and T. Merriman

*Contract No. NAS8-33576*

August 20, 1980

BATTELLE  
COLUMBUS LABORATORIES  
505 KING AVENUE  
COLUMBUS, OHIO 43201

TABLE OF CONTENTS

	<u>Page</u>
INTRODUCTION. . . . .	1
SUMMARY . . . . .	2
ANALYSIS DETAILS. . . . .	3
Method of Computation. . . . .	3
BASDAP Computer Model . . . . .	3
Tribological Inputs . . . . .	4
Outer-Race Hoop Stress Computations . . . . .	9
Ball-Cage Stresses. . . . .	9
Estimate of Internal Bearing Temperature. . . . .	13
Bearing Crush Load Calculations . . . . .	17
Results of Computations. . . . .	18
Outer Race Stress Computations. . . . .	18
Cage Stresses . . . . .	23
Heating Calculations. . . . .	24
Bearing Life. . . . .	24
Crush Load Estimates. . . . .	25
Calculating Units. . . . .	25
REFERENCES. . . . .	26

APPENDIX A

DATA ON AISI 440C STAINLESS STEEL . . . . .	A-1
---------------------------------------------	-----

TABLE OF CONTENTS  
LIST OF TABLES

	<u>Page</u>
Table 1. Basic Bearing Parameters. . . . .	19
Table 2. Summary of Computations for High Pressure Oxygen Turbopump Bearings, Case No. 07955, Turbine End .	20
Table 3. Summary of Computations for High Pressure Oxygen Turbopump Bearings, Case No. 07958, Pump End. . .	21
Table 4. Summary of Computations for High Pressure Fuel Turbopump Bearings, Case No. 07502. . . . .	22

LIST OF FIGURES

Figure 1. Schematic Drawing of Solid-Film Ball-Bearing Simulator. . . . .	5
Figure 2. Typical Normal Force Versus Slip Data for Teflon Transfer Film . . . . .	7
Figure 3. Effect of Ball-Cage Load on Ball-Cage Traction . .	8
Figure 4. Nomenclature for Outer Race Hoop Stress Calculations . . . . .	10
Figure 5. Nomenclature for Cage Hoop Stress Calculations . .	12
Figure 6. Nomenclatures for Bearing Thermal Calculations . .	14
Figure 7. Simplified Model of Ball-Race Contact. . . . .	15

# SSME TURBOPUMP BEARING ANALYTICAL STUDY

by

J.W. Kannel and T. Merriman

## INTRODUCTION

NASA is currently involved in the development and evaluation of long-life turbopumps for use on the shuttle spacecraft main engine (SSME). Because of the reusable design of the shuttle, lifetimes of 27,000 seconds (7.5 hours) are being sought, whereas most turbopumps to date have only operated for periods on the order of a few hundred seconds. While all components are being considered in efforts to achieve a satisfactory design, the turbopump support bearings are of particular concern. Battelle's Columbus Laboratories is supporting NASA in the area of bearing failure and dynamic analyses. This particular task deals with an analytical evaluation of three engine bearings operating under severe overspeed and shut-down conditions.

The specific questions addressed in this task were with regard to:

- Outer race stresses
- Cage stresses
- Cage-race drag
- Bearing heating
- Crush loading.

The analyses were based on the use of a Battelle bearing dynamics computer model BASDAP II. This model computes ball-race forces and dynamic motions. The model was modified to enable estimating the various stresses requested by this task.

SUMMARY

Numerous computations of bearing life-critical parameters have been performed for three shuttle pump bearings (two for the high pressure oxygen pump and one for the high pressure fuel pump). These computations were performed for very severe bearing operating conditions. The following predictions for limiting conditions were made for momentary overspeed and overload, assuming a 17,800 N (4000 pounds) axial load on the bearing:

Pump	Bearing	Bearing Drawing Number	Speed, rpm	Radial Load Total On Two Bearings	Probable Problem
Oxygen	Turbine End	7955	36,000 or higher	26,700 N (6000 pounds)	Cage Failure
Oxygen	Turbine End	7955	30,000 or higher	35,600 N (8000 pounds)	Cage Failure
Oxygen	Pump End	7958	30,000 or higher	26,700 N (6000 pounds)	Cage Failure
Oxygen	Pump End	7958	30,000 or higher	35,600 N (8000 pounds)	Cage Failure
Fuel	---	7502	30,000 or higher	26,700 N (6000 pounds)	Cage Failure
Fuel	---	7502	30,000 or higher	35,600 N (8000 pounds)	Cage Failure

Generally, radial loads on the order of 13,300 N (3000 pounds) per bearing or 26,700 N (6000 pounds) per bearing pair, could be expected to cause severe problems to any of these bearings with a 17,800 N (4000 pounds) axial load. Further, when possible temperature excursions are considered, even a load of 8900 N (2000 pounds) may be excessive. However, high momentary radial loads with a 3800 N (850 pounds) axial load would not be anticipated to cause catastrophic failure of the fuel pump bearing.

These calculations are based on the assumption of very severe short-term external forces on the bearings in order to explore the typical likely failures. However, we believe all conditions considered were far too severe for the bearings in terms of expecting long-term reliable service. Even if a gross failure does not occur during the load application, overall life is likely to be compromised. On this basis, efforts should be made to avoid the high loads entirely.

## ANALYSIS DETAILS

### Method of Computation

#### BASDAP Computer Model

The method for bearing load computations at Battelle involves the use of a computer program under the general name, BASDAP. BASDAP programs can be used for static or dynamic analyses of bearings for a wide range of applications. For example, BASDAP programs have been used in:

- (1) Static or quasi-dynamic analyses to determine ball-race stresses and ball steady-state motions
- (2) Determining the effects of unusual load conditions, such as staggered ball spacings
- (3) Analyses of dynamic behavior of the cage to determine cage stability and ball-cage loadings.

The BASDAP program treats each bearing in a set independently.

For the project discussed herein, a quasi-dynamic version of the BASDAP computer code was utilized. This code involves calculation of ball-race forces (inner and outer), contact pressures, contact dimensions, and contact angles as a function of (1) axial load, (2) radial load, and (3) centrifugal load on the bearing.

The computation technique involves first computing the load sharing between the balls in the absence of centrifugal forces. This involves a formalized trial and error (nesting type) procedure. Estimates of the axial and radial deflections of the bearings are made and the correct value of these deflections results in the correct radial and axial load. After the ball load sharing has been computed, the effect of centrifugal forces on contact angle is computed. This force causes the inner and outer race contact angles to be different from each other as well as different from the static contact angles. The method for the deflection and contact angles calculation is modeled after the classic work of A.B. Jones [1]\*.

### Tribological Inputs

One of the most critical aspects of the BASDAP model is the force computations at the ball-race and ball-cage interfaces. For a liquid-lubricated bearing, these forces are modeled by elastohydrodynamic (EHD) theory. However, the shuttle bearings are not liquid lubricated, but are intended to be lubricated with a Teflon transfer film. This transfer film behaves more like a solid interface than a liquid and at this stage in time is not well understood. Some progress is being made in this area in another research project at Battelle. For that project, a solid-film ball-bearing simulator has been constructed to study the interface conditions. Essentially, the ball-bearing simulator consists of a bearing ball sandwiched between two motor-drive inner races (see Figure 1). The ball is located by a cage segment mounted in an adjustable frame. The frame is restrained by a multi-axis load cell, which detects normal and friction forces. Ball-cage friction is monitored by the tangential force transducer and ball-race friction is monitored by the normal force transducer. In the experiments with this bearing simulator,

---

\*References are listed on page 26.



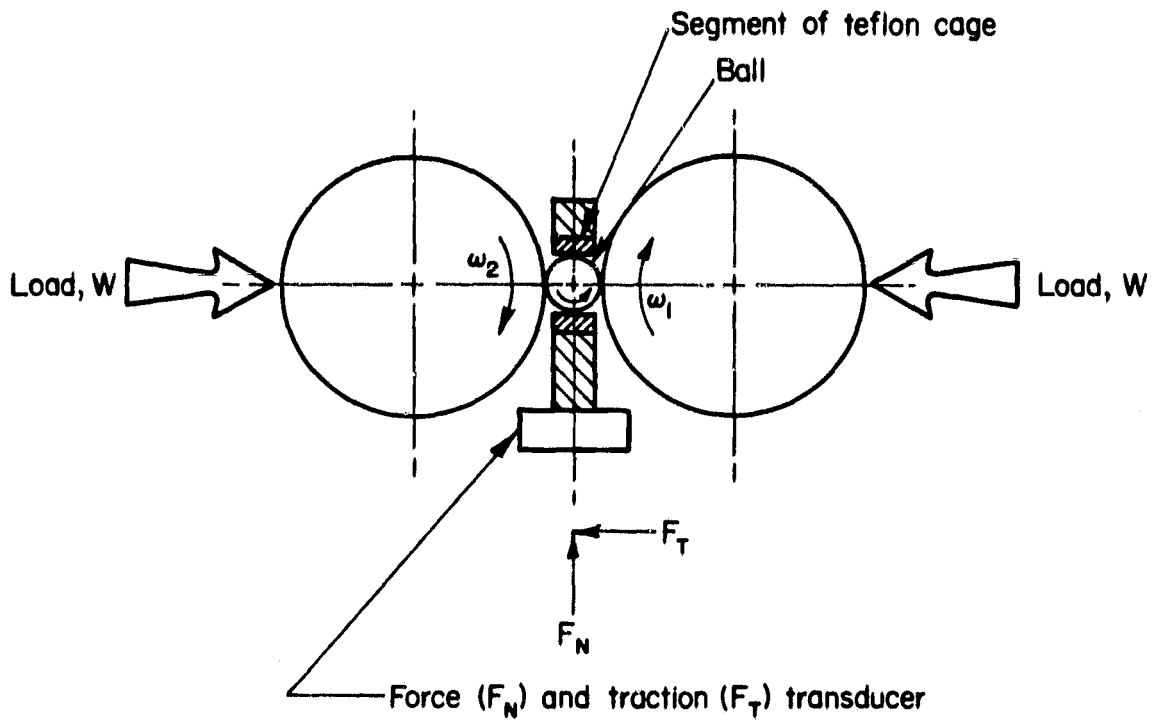


FIGURE 1. SCHEMATIC DRAWING OF SOLID-FILM BALL-BEARING SIMULATOR

the system is operated for a sufficient time to form a Teflon transfer film from the cage segment to the ball and in turn, to the races. The tests consist of the measurement of normal and tangential forces as a function of slip  $(\omega_1 - \omega_2)$  between the races for a given load between the races.

Figure 2 shows normal-force versus slip data for a Teflon transfer film at two load conditions. As can be observed at low-slip conditions, force depends on the level of slip. However, at higher slip conditions, the data show an asymptote which corresponds to friction coefficients,  $f_1$ , of 0.14 for a ball between two races. This value of  $f$  was used in the computations to determine ball-cage forces. That is, if the force on a ball was, say, 1000 N (225 pounds), then the maximum cage force would be 140 N (31 pounds).

The shape of the curve for Figure 2 was modeled in the form<sup>[2]</sup>

$$F_N = C_1 \tan^{-1} (C_2 \Delta\omega) \quad , \quad (1)$$

to allow for the ball-spin and ball-cage force calculations in the BASDAP program. Here, the  $C_1$  and  $C_2$  parameters are used to fit the data of Figure 2. As an example, the data of Figure 2

$$F_N = 0.090 W \tan^{-1} \left( 0.12 \frac{\Delta\omega}{2} \right) \text{ (Newtons)} \quad , \quad (2)$$

where  $\frac{\Delta\omega}{2}$  is the slip at either of the two ball-race interfaces and  $W$  is the total loading. The normal force at either of the two ball and contacts would be assumed to be  $\frac{F_N}{2}$ .

A typical ball-cage friction curve is shown in Figure 3. These data were obtained using the traction measurement capability from the ball-bearing simulator. For this condition, it was estimated that the ball-cage friction coefficient was about 0.25.

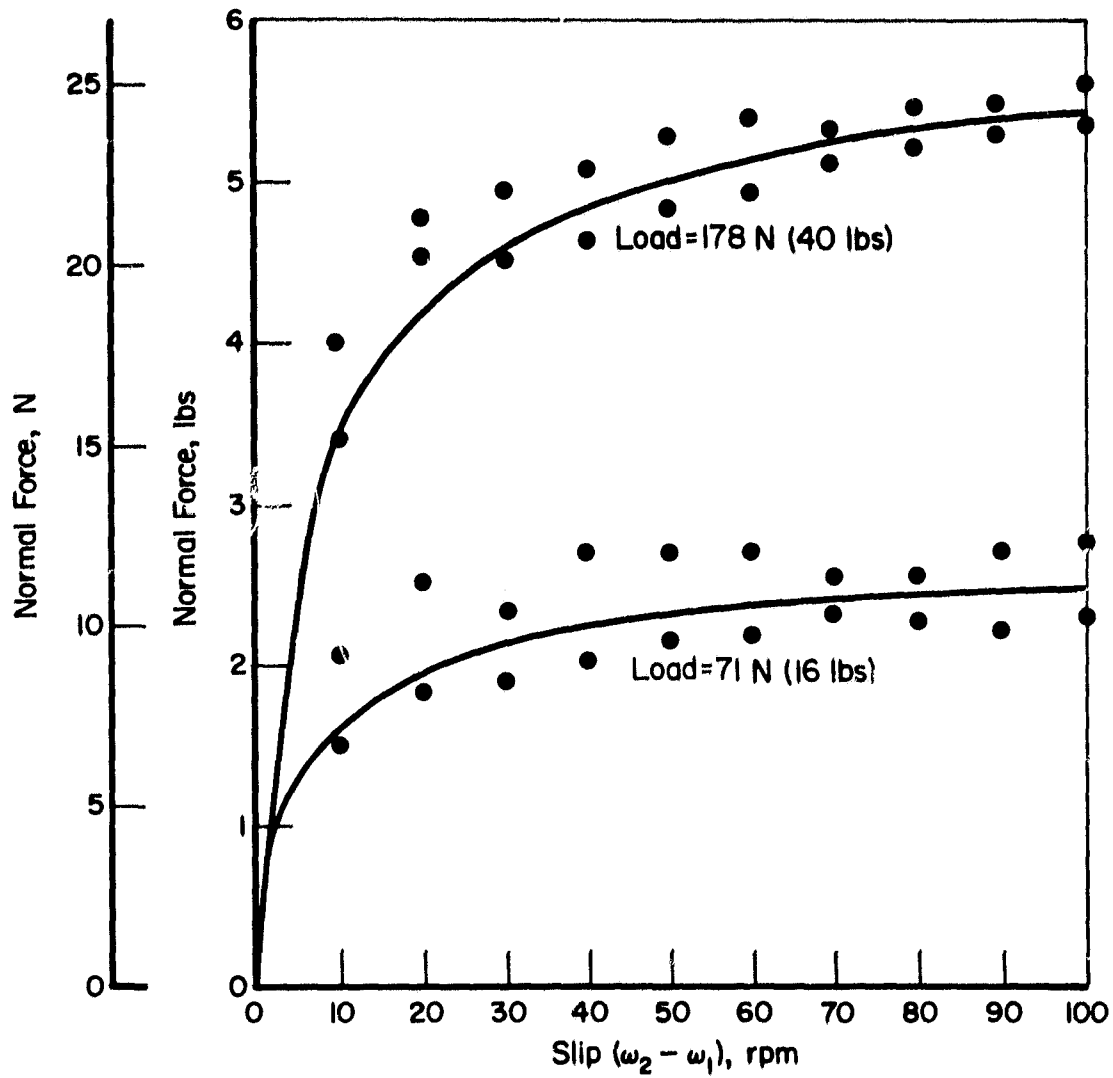


FIGURE 2. TYPICAL NORMAL FORCE VERSUS SLIP DATA FOR TEFLON TRANSFER FILM



### Outer-Race Hoop Stress Computations

The method for computing the hoop stress in the bearing outer race involved balancing the ball-race loading (from the BASDAP model) with the outer race stresses. The bearing loading for the BASDAP model was defined so that the ball load would be symmetrical about the y axis. For this case, the hoop stress,  $\sigma_{HR}$ , can be given by (see Figure 4)

$$\sigma_{HR} = \frac{1}{2 \cdot A_{race}} \sum_{\theta=0}^{\theta=\pi} F_{BO} \cos \beta_o \sin \theta \quad , \quad (3)$$

where  $F_{BO}$  is the load between ball and race,  $\beta_o$  is the outer contact angle, and  $A_{race}$  is the cross-sectional area of the race.

### Ball-Cage Stresses

Ball-Cage Forces. Cage forces are difficult to predict for a bearing operating under the extreme conditions existing in the shuttle turbopump system. The extreme values of the forces occur when one ball is pushing the cage against another ball. Here, the ball-cage force would be the inner-outer ball-race friction coefficient ( $\sim 0.14$ ) times the ball-race load. Under axial loads or moderately low radial loads, the probability of the cage being so loaded is small. However, under a large ratio of radial to axial load, ball-speed-variation (BSV) can cause these extreme cage loads to occur. Good bearing design would require the cage to be able to withstand the extreme loads even if this probability of occurrence is very low. If this type of design is not practical for all operating conditions of a bearing, it is mandatory that radial loads in the bearing be controlled to eliminate the possibility of severe BSV problems.

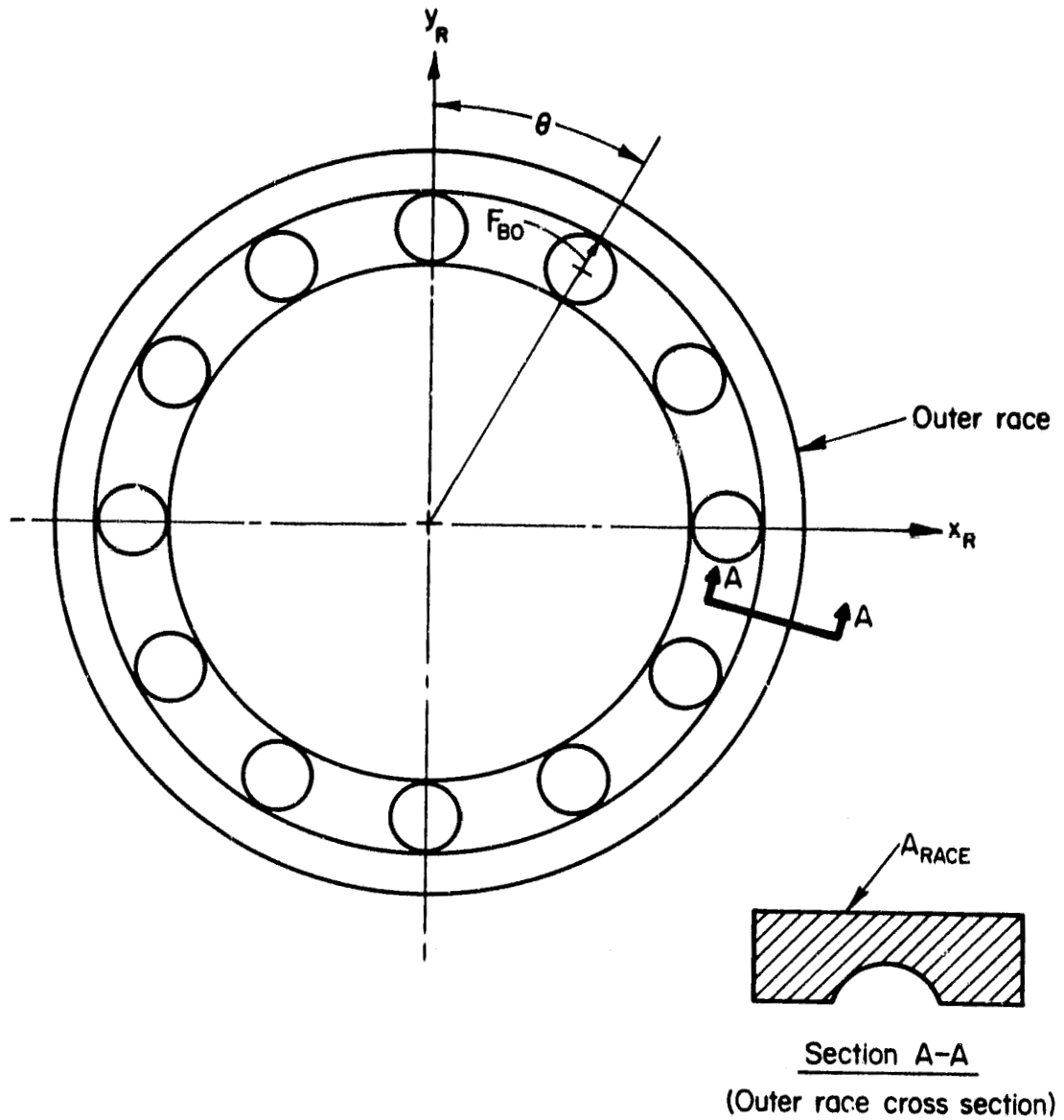


FIGURE 4. NOMENCLATURE FOR OUTER RACE  
HOOP STRESS CALCULATIONS

In the BASDAP calculations, the ball-cage forces were computed using the tribological arctangent model discussed earlier. For this model, no radial load implies a very low cage force. However, even a small radial load results in significant force predictions because of the difficulty balls have in slipping on the transfer film. For the resulting cage stresses, a summation of the average force from each ball contact was used and this force was normally very high. Also, the contribution of the BSV of the balls was computed. If these excursions were less than the ball-pocket diametral clearance, the probability of the force being applied to the cage was considered low. Conversely, if the excursion exceeded the clearance, then the probability of ball-cage force was high and cage failure or extreme wear would be likely.

Cage Hoop Stress. For these computations, the cage was modeled as shown in Figure 5. The ball-cage forces,  $F_{BC}$ , are assumed to be identical and are balanced by a force of  $2 F_{BC}$  at the cage-race contact. As a result of these forces, a tensile stress at point A occurs and is given by<sup>[3]</sup>

$$\sigma_{AC} = 0.636 \frac{F_{BC}}{A_C} \left( 1 + \frac{1}{Z} \frac{y}{R_p + y} \right) , \quad (4)$$

$$\text{where } Z = -1 + \frac{R_p}{T_c} \ln \left( \frac{R_p + c}{R_p - c} \right).$$

Here  $\sigma_{AC}$  = cage hoop stress

$R_p$  = pitch radius

$T_c$  = cage thickness

$c = T_c/2$

$A_C$  = effective area on the cage

$[W_{TH} \cdot T_c \text{ or } (W_{TH} - 2 R_{poc}) \cdot T_c]$

$y = \pm c$  is the location of the stress

$W_{TH}$  = cage width

$R_{poc}$  = radius of pocket.

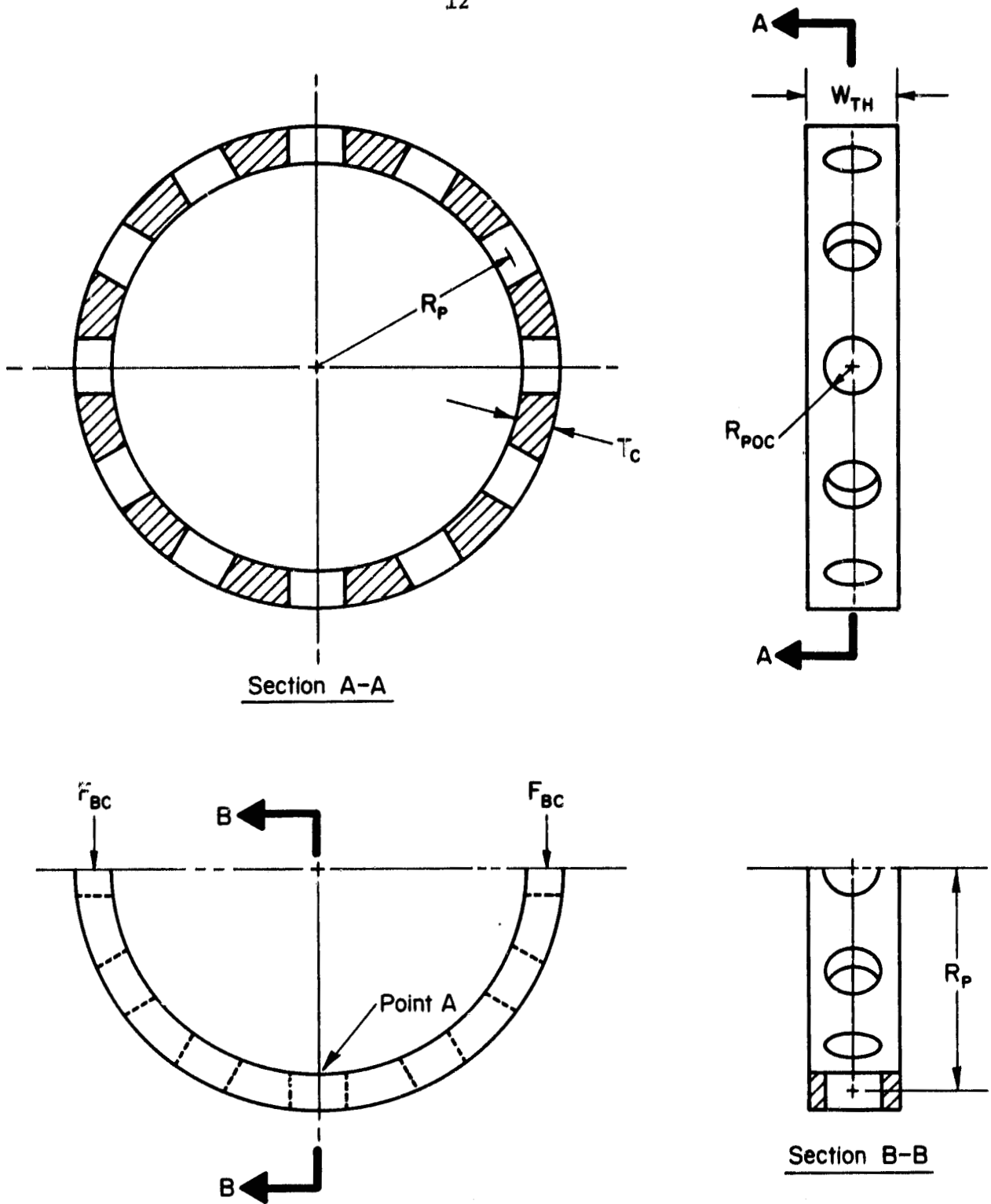


FIGURE 5. NOMENCLATURE FOR CAGE HOOP STRESS CALCULATIONS



Ball-Cage Compressive Forces. The ball-cage compressive forces were computed using the average ball-cage force,  $F_{BC}$ , in conjunction with Hertz contact stress theory[4].

Cage-Race Friction Force. The cage-race friction force was estimated as twice the ball-cage force times the coefficient of friction at the cage-race interface.

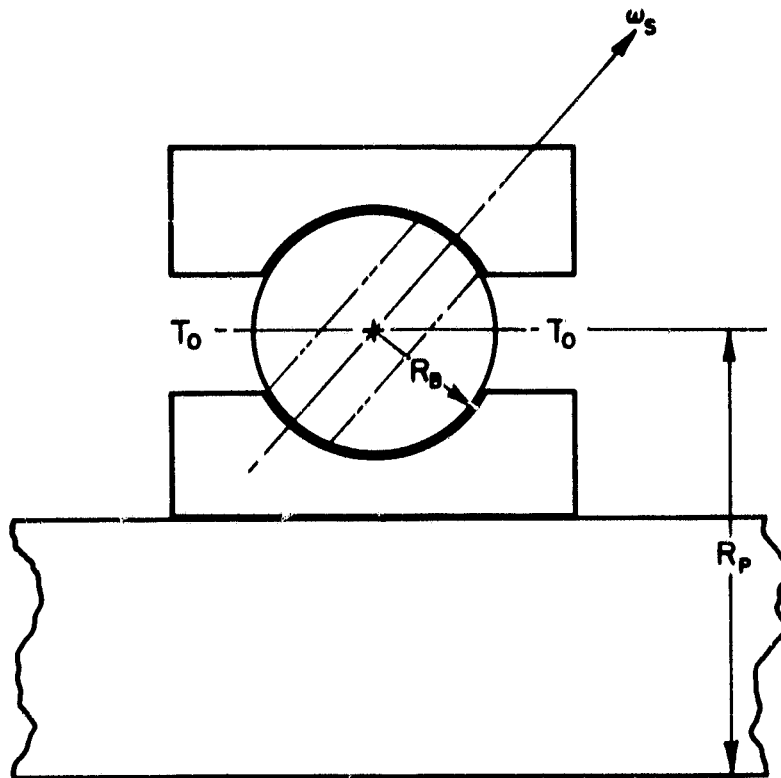
#### Estimate of Internal Bearing Temperature

The turbopump bearings represent rather unique situations with regards to bearing temperatures. Sizeable heat can be generated at the ball-race contact as a result of ball-spinning on the solid transfer film (see Figure 6). However, the cryogenic fluids represent a very good external thermal environment for the balls.

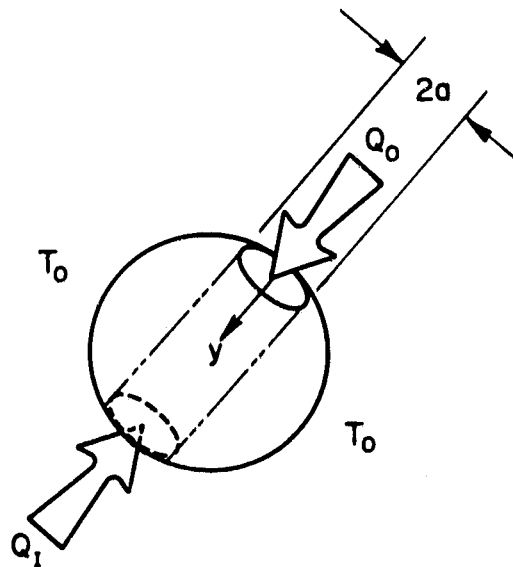
Heat Generation. As discussed in the tribological input section, it appears that the transfer film can be represented by a constant friction coefficient interface. Further, we can assume that the Hertzian contact can be represented by a rectangle with dimensions  $\sqrt{\pi} a$  and  $\sqrt{\pi} b$  under a constant pressure  $P_{ave}$  (see Figure 7). With these assumptions, the load,  $P_L$ , would be

$$P_L = P_{ave} (\sqrt{\pi} a) (\sqrt{\pi} b) = P_{ave} \pi ab \quad , \quad (5)$$

which is consistent with Hertz theory. Here,  $a$  and  $b$  are the major and minor axes of the contact ellipse and  $P_{ave} = \frac{2}{3} P_o$ , where  $P_o$  is the maximum Hertz pressure.



a. Bearing Nomenclature



b. Ball Heating Nomenclature

FIGURE 6. NOMENCLATURES FOR BEARING THERMAL CALCULATIONS

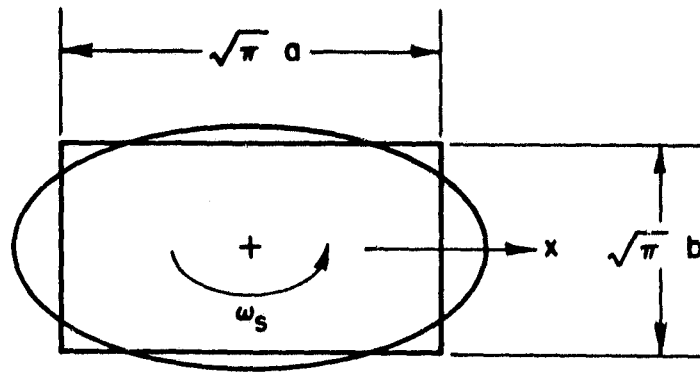


FIGURE 7. SIMPLIFIED MODEL OF BALL-RACE CONTACT

The heat generation for this contact can be written

$$Q = \frac{2}{A_R} \int_0^{\frac{\sqrt{\pi} a}{2}} f P_{ave} \sqrt{\pi} b \omega_S x \, dx \quad , \quad (6)$$

where  $A_R$  is the effective area for heat transfer for each ball.

$$Q = \frac{0.93 f P_O \omega_S b a^2}{A_R} \quad . \quad (7)$$

Because of the high speed of the bearing, it is reasonable for heat computations that the ball track be represented by a thin disk with a radius equivalent to the ball pitch radius with a width of  $2a$  or

$$A_R = 4\pi \frac{R_p a}{N_B} \quad , \quad (8)$$

where  $N_B$  is the number of balls.

Using Equation (8), Equation (7) can be written

$$Q = 0.074 f P_O \frac{\omega_S b a N_B}{R_p} \quad , \quad (9)$$

where  $Q$  is the heat input at the inner or outer race ball contact zone.

Heat Transfer to Ball. By assuming the thin disk model for heat transfer in the ball region, the heat transfer can be written

$$\frac{\partial^2 T}{\partial x^2} + \frac{\partial^2 T}{\partial y^2} = 0 \quad , \quad (10)$$

where the boundary conditions are  $T(0,y) = T(2a,y) = 0$ .

$$\frac{\partial T}{\partial y} (x, 0) = -q_0 \quad , \quad (11)$$

$$\frac{\partial T}{\partial y} (x, 2R_B) = +q_i \quad ,$$

where  $q_0$  and  $q_i$  are the temperature gradients of the inner and outer races.

A solution could be written

$$T = \sum \left( C_1 e^{\lambda y} + C_2 e^{-\lambda y} \right) \sin \frac{n\pi x}{2a} \quad , \quad (12)$$

where  $\lambda = \frac{n\pi}{2a}$  and  $T$  is the temperature rise above the surrounding atmosphere. Note that

$$q_i = \frac{Q_i}{2K} \text{ and } q_0 = \frac{Q_0}{2K} \quad , \quad (13)$$

where  $K$  is thermal conductivity and it is assumed that half of the heat enters the ball and half enters the race.

The maximum temperature at the inner and outer race contacts can be written approximately as

$$T_{mx}(\text{inner}) = 0.48 \frac{aQ_0}{K} \quad ,$$

$$T_{mx}(\text{outer}) = 0.48 \frac{aQ_i}{K} \quad , \quad (14)$$

where  $K$  is thermal conductivity equals 0.00698 Kcal meter/meter<sup>2</sup>sec °C (3.65 ft lbs/sec ft °F) for 440C stainless steel (see Appendix A).

### Bearing Crush Load Calculations

Under extreme load conditions, the balls and/or race may fail completely due to excessive stresses. One method to estimate this extreme (crush) load is to use an ultimate yield criteria such as the von-Mises

criteria<sup>[5]</sup> which states that  $\sigma_{ULT} = 3Y$ , where  $Y$  is the yield stress and  $\sigma_{ULT}$  is the ball compressive stress. For 440C (see Appendix A),  $Y = 1.9$  GPa (275,000 psi). If  $\sigma_{ULT}$  is based on the maximum Hertz ball-race contact pressure, then  $P_0$  (ultimate) = 5.7 GPa (825,000 psi), or if  $\sigma_{ULT}$  is based on the mean Hertz stress, then  $P_0$  (ultimate) = 8.5 GPa (1,230,000 psi).

### Results of Computations

By using the methods described above, computations were conducted for the three separate bearing configurations. The bearing data used are shown in Table 1, and the results are summarized in Tables 2 through 4 for the three bearing configurations. Tables 2 and 3 are for the high pressure oxidizer turbopump bearing and are consistent with the matrix of conditions requested. Computations were not possible for the last four cases in Table 3 because the conditions exceeded the computer model capabilities. Table 4 (Fuel Turbopump bearing) was intended to show bearing stresses under momentary radial loads during shut-down conditions and transient overloads.

### Outer Race Stress Computations

The compressive stresses are within crush load limits for all cases considered. However, peak stresses of 3.64 GPa (524,000 psi) are very extreme for a transfer film bearing and will doubtless cause excessive wear and poor life as evidenced by the life predictions. Since transfer films are inadequate above about 2 GPa (300,000 psi) maximum stress, bearing performance will be very poor. The hoop stresses in the bearing do not appear to be excessive in comparison with the tensile yield of 440C (see Appendix A). However, these stresses are accompanied by a race elastic growth, which could cause jamming of the outer race.

TABLE 1. BASIC BEARING PARAMETERS

Parameter	Symbol	Units	Oxygen Pump Bearing		High Pressure
			Turbine End 007955	Pump End 007958	Fuel Pump Bearing 007502
Radius of Pitch	$R_p$	Inches	1.595	1.280	1.170
Ball Radius	$R_B$	Inches	.25	.21875	.17375
Contact Angle	$\beta_{\bar{d}}$	rad/degrees	.36/20.5	.43/25.	.48/28.
Inner Curvature	F	---	.53	.53	.53
Outer Curvature	F	---	.53	.52	.52
Number of Balls	$N_B$	---	13	13	14
Bearing Fit (Dia.)	DIR	Inches	-.003	-.003	-.003
Radius of Ball Pocket	$R_{poc}$	Inches	.262	.236	.184
Cage Thickness	THK	Inches	.175	.170	.122
Cage-Race Clearance	$C_{CR}$	Inches	.02/.027	.0045/.0115	.0045/.0115
Cage Width	$W_{TH}$	Inches	.736	.655	.574

TABLE 2. SUMMARY OF COMPUTATIONS FOR HIGH PRESSURE OXYGEN TURBOPUMP BEARINGS,  
CASE NO. 07955, TURBINE END, AT AN AXIAL LOAD OF 17,800 N (4000 POUNDS)

Radial Load Per Pair (N(lbs))	Speed, rpm	Race Stresses (GPa/Ksi)						Maximum Cage Stresses (GPa/Ksi)					Cage-Race Drag (N(lbs))	Maximum Temperature Rise (°C/°F)				L <sub>10</sub> Life, seconds	
		Inner Compressive		Outer Compressive		Outer Hoop	Pocket Compressive	Hoop Stress	Prob-ability	Inner Race	Outer Race								
0	30,000	2.87	413.	2.64	379.	.060	8.65	.001	.2	NIL	Low	NIL	24.	43.	95.	170.	833.		
0	32,000	2.85	411.	2.65	381.	.061	8.78	.002	.3	NIL	Low	NIL	20.	36.	106.	191.	789.		
0	34,000	2.84	410.	2.66	383.	.062	8.91	.003	.4	NIL	Low	NIL	15.	28.	119.	213.	748.		
0	36,000	2.83	408.	2.67	385.	.063	9.06	.003	.4	NIL	Low	NIL	10.	18.	132.	238.	712.		
0	38,000	2.82	406.	2.69	387.	.064	9.22	.003	.5	NIL	Low	NIL	3.	6.	147.	264.	678.		
8900/2000	30,000	3.09	445.	2.81	405.	.060	8.63	.190	27.4	.378	54.5	Low	134.	30.1	40.	72.	115.	207.	745.
"	32,000	3.08	444.	2.82	406.	.061	8.76	.194	27.9	.397	57.2	Low	141.	31.6	37.	66.	128.	230.	705.
"	34,000	3.07	442.	2.83	408.	.062	8.90	.194	28.0	.403	58.0	Low	142.	32.0	32.	58.	142.	255.	668.
"	36,000	3.06	441.	2.84	409.	.063	9.04	.196	28.2	.409	58.9	Low	145.	32.5	21.	49.	157.	282.	635.
"	38,000	3.05	439.	2.85	411.	.064	9.20	.197	28.3	.416	59.9	High	147.	33.1	37.	173.	312.	604.	
17800/4000	30,000	3.30	475.	2.98	429.	.060	8.64	.193	27.8	.395	56.9	Low	140.	31.4	58.	105.	136.	245.	580.
"	32,000	3.29	474.	2.99	430.	.061	8.76	.195	28.1	.406	58.5	Low	144.	32.4	56.	100.	151.	272.	548.
"	34,000	3.28	472.	2.99	431.	.062	8.90	.197	28.4	.419	60.3	Low	149.	33.4	52.	94.	167.	300.	519.
"	36,000	3.27	471.	3.01	433.	.063	9.05	.199	28.7	.433	62.4	Low	153.	34.5	47.	85.	184.	331.	493.
"	38,000	3.26	470.	3.01	434.	.064	9.21	.199	28.7	.435	62.6	Low	154.	34.6	42.	74.	202.	363.	469.
26700/6000	30,000	3.49	503.	3.13	451.	.060	8.66	.194	27.9	.396	57.0	Low	140.	31.5	78.	141.	160.	287.	421.
"	32,000	3.48	501.	3.14	452.	.061	8.79	.196	28.2	.413	59.4	Low	146.	32.8	77.	139.	176.	317.	397.
"	34,000	3.47	500.	3.15	453.	.062	8.93	.197	28.4	.422	60.7	Low	149.	33.5	74.	134.	193.	348.	376.
SEVERE FAILURE																			
26700/6000	36,000	3.47	499.	3.16	455.	.063	9.08	.198	28.5	.422	60.8	High	149.	33.6	71.	127.	212.	382.	358.
"	38,000	3.46	498.	3.17	456.	.064	9.24	.198	28.5	.423	60.9	High	150.	33.7	65.	118.	232.	418.	340.
35600/8000	30,000	3.67	529.	3.29	473.	.060	8.71	.194	27.9	.397	57.1	High	141.	31.6	101.	181.	184.	331.	300.
"	32,000	3.67	528.	3.29	474.	.061	8.84	.195	28.1	.407	58.6	High	144.	32.4	101.	181.	202.	364.	283.
"	34,000	3.66	527.	3.30	475.	.062	8.99	.196	28.2	.409	58.9	High	145.	32.6	99.	176.	222.	399.	268.
"	36,000	3.65	526.	3.31	476.	.063	9.14	.196	28.2	.411	59.2	High	145.	32.7	96.	173.	242.	435.	254.
"	38,000	3.64	524.	3.31	477.	.065	9.31	.197	28.3	.414	59.6	High	147.	33.0	92.	165.	264.	476.	242.



TABLE 3. SUMMARY OF COMPUTATIONS FOR HIGH PRESSURE OXYGEN TURBOPUMP BEARINGS,  
CASE NO. 07958, PUMP END, AT AN AXIAL LOAD OF 17,800 N (4000 POUNDS)

Radial Load Per Pair (N(lbs))	Speed, rpm	Race Stresses (GPa/Ksi)					Maximum Cage Stresses (GPa/Ksi)					Cage-Race Drag (N(lbs))	Maximum Temperature Rise (°C/°F)				L <sub>10</sub> Life, seconds		
		Inner Compressive		Outer Compressive		Outer Hoop	Pocket Compressive		Hoop Stress	Probability	Inner Race		Outer Race						
0	30,000	3.06	440.	2.49	358.	.055	7.91	.002	.347	NIL	Low	NIL	31.5	56.7	86.	155.	661.		
0	32,000	3.05	439.	2.49	359.	.055	7.99	.002	.317	NIL	Low	NIL	29.7	53.4	94.	170.	625.		
0	34,000	3.05	439.	2.50	361.	.056	8.07	.002	.269	NIL	Low	NIL	27.1	48.8	103.	186.	594.		
0	36,000	3.04	438.	2.51	362.	.057	8.17	.001	.171	NIL	Low	NIL	23.9	43.8	113.	203.	567.		
0	38,000	3.03	437.	2.52	363.	.057	8.27	.002	.228	NIL	Low	NIL	20.0	36.0	123.	222.	542.		
8960/2000	30,000	3.33	479.	2.69	388.	.055	7.89	.002	.307	.322	46.3	Low	116.	26.1	49.7	89.5	111.	199.	578.
"	32,000	3.33	479.	2.70	389.	.055	7.97	.216	31.1	.334	48.1	Low	121.	27.2	48.6	87.5	121.	217.	545.
"	34,000	3.32	478.	2.70	389.	.056	8.06	.219	31.5	.348	50.1	Low	126.	28.3	46.8	84.3	131.	236.	519.
"	36,000	3.31	477.	2.71	390.	.057	8.15	.219	31.6	.353	50.8	Low	128.	28.7	44.2	79.6	142.	256.	492.
"	38,000	3.31	477.	2.72	391.	.057	8.25	.221	31.8	.358	51.5	Low	129.	29.1	40.8	73.4	154.	278.	471.
17800/4000	30,000	3.58	515.	2.88	415.	.055	7.90	.217	31.3	.340	49.0	Low	123.	27.7	70.0	126.	137.	247.	423.
"	32,000	3.57	515.	2.88	415.	.055	7.98	.219	31.5	.349	50.2	Low	126.	28.4	70.0	126.	149.	268.	399.
"	34,000	3.57	514.	2.89	416.	.056	8.07	.221	31.8	.358	51.5	Low	129.	29.1	69.4	125.	161.	290.	379.
"	36,000	3.56	513.	2.90	417.	.057	8.16	.223	32.1	.367	52.9	Low	133.	29.9	67.8	122.	174.	314.	360.
"	38,000	3.56	513.	2.90	418.	.057	8.26	.225	32.4	.378	54.4	Low	137.	30.7	65.0	117.	188.	339.	344.
<b>SEVERE FAILURE</b>																			
26700/6000	30,000	3.81	548.	3.05	440.	.055	7.94	.217	31.3	.342	49.3	High	124.	27.9	92.8	167.	165.	297.	289.
"	32,000	3.81	548.	3.06	440.	.056	8.03	.220	31.7	.355	51.1	High	129.	28.9	93.3	168.	179.	322.	273.
"	34,000	3.80	547.	3.06	441.	.056	8.11	.223	32.1	.368	53.0	High	133.	30.0	93.9	169.	193.	348.	258.
"	36,000	3.79	546.	3.07	442.	.057	8.21	.224	32.2	.371	53.4	High	134.	30.2	93.3	168.	208.	375.	245.
"	38,000	3.79	546.	3.07	442.	.058	8.31	.224	32.2	.373	53.7	High	135.	30.3	91.7	165.	224.	403.	234.
35600/8000	30,000	4.02	579.	3.22	463.	.056	8.01	.219	31.5	.349	50.2	High	126.	28.4	116.7	210.	194.	350.	197.
"	32,000	COMPUTER PROGRAM WOULD NOT RUN																	
"	34,000	COMPUTER PROGRAM WOULD NOT RUN																	
"	36,000	COMPUTER PROGRAM WOULD NOT RUN																	
"	38,000	COMPUTER PROGRAM WOULD NOT RUN																	

TABLE 4. SUMMARY OF COMPUTATIONS FOR HIGH PRESSURE FUEL TURBOPUMP BEARING,  
CASE NO. 07502

Axial Load, (N(lbs))	Radial Load Per Pair (N(lbs))	Speed, rpm	Race Stresses (GPa/Ksi)						Maximum Cage Stresses				Cage-Race Drag (N(lbs))	Maximum Temperature Rise (°C/°F)				L <sub>10</sub> Life, seconds		
			Inner Compressive		Outer Compressive		Outer Hoop	Pocket Compressive	Hoop Stress	Prob-ability	Inner Race	Outer Race								
17800/4000	0	30,000	3.51	506.	2.88	414.	.088	12.7	.003	.457	NIL	Low	NIL	50.9	91.6	93.8	167.	175.		
"	0	32,000	3.51	506.	2.88	415.	.089	12.8	.003	.453	NIL	Low	NIL	51.4	92.6	101.	181.	164.		
"	0	34,000	3.51	506.	2.88	415.	.090	12.9	.003	.446	NIL	Low	NIL	51.5	92.7	109.	196.	156.		
"	0	36,000	3.51	505.	2.89	416.	.090	13.0	.003	.435	NIL	Low	NIL	51.1	91.9	117.	211.	148.		
"	0	38,000	3.50	505.	2.89	416.	.090	13.0	.003	.428	NIL	Low	NIL	50.1	90.1	126.	227.	141.		
"	8900/2000	30,000	3.82	550.	3.11	448.	.088	12.7	.247	35.6	.535	77.1	Low	121.	27.3	72.8	131.	119.	215.	155.
"	"	32,000	3.81	549.	3.11	448.	.088	12.7	.249	35.9	.549	79.0	Low	124.	27.9	74.4	134.	129.	233.	146.
"	"	34,000	3.81	549.	3.12	449.	.089	12.8	.251	36.2	.562	80.9	Low	127.	28.6	75.6	136.	139.	251.	138.
"	"	36,000	3.81	548.	3.12	449.	.090	12.9	.253	36.5	.576	82.9	Low	130.	29.3	76.1	137.	150.	270.	131.
"	"	38,000	3.80	548.	3.12	450.	.090	12.9	.256	36.8	.590	85.0	Low	133.	30.0	76.1	137.	161.	289.	124.
"	17800/4000	30,000	4.09	589.	3.32	478.	.088	12.6	.254	36.6	.581	83.6	Low	132.	29.6	96.1	173.	148.	267.	117.
"	"	32,000	4.08	588.	3.32	479.	.088	12.6	.256	36.8	.589	84.8	Low	133.	30.0	99.4	179.	160.	288.	110.
"	"	34,000	4.08	588.	3.33	479.	.088	12.7	.257	37.0	.598	86.1	Low	135.	30.4	101.	183.	172.	309.	104.
"	"	36,000	4.08	587.	3.33	480.	.089	12.8	.258	37.2	.608	87.5	Low	137.	30.9	103.	186.	184.	332.	98.
"	"	38,000	4.08	587.	3.33	480.	.090	12.9	.260	37.4	.617	88.9	Low	140.	31.4	105.	189.	197.	355.	94.
"	26700/6000	30,000	4.33	624.	3.52	507.	.087	12.5	.253	36.4	.571	82.2	High	129.	29.1	121.	217.	178.	320.	82.
"	"	32,000	4.33	624.	3.52	507.	.088	12.6	.255	36.7	.584	84.1	High	132.	29.7	125.	225.	191.	344.	77.
"	"	34,000	4.33	624.	3.52	507.	.088	12.6	.257	37.0	.598	86.1	High	135.	30.4	129.	232.	205.	369.	73.
"	"	36,000	4.33	623.	3.53	508.	.088	12.7	.259	37.3	.613	88.2	High	139.	31.2	132.	238.	219.	395.	69.
"	"	38,000	4.33	624.	3.53	508.	.089	12.8	.261	37.6	.628	90.4	High	142.	32.0	135.	243.	234.	422.	66.
"	35600/8000	30,000	4.56	657.	3.69	533.	.086	12.4	.252	36.3	.563	81.1	High	128.	28.7	145.	261.	207.	372.	58.
"	"	32,000	4.56	657.	3.70	533.	.086	12.4	.254	36.6	.581	83.7	High	132.	29.6	151.	272.	222.	399.	54.
"	"	34,000	4.56	657.	3.70	533.	.087	12.5	.257	37.0	.601	86.5	High	136.	30.6	156.	238.	238.	428.	51.
"	"	36,000	4.56	656.	3.71	534.	.088	12.6	.259	37.3	.615	88.6	High	139.	31.3	161.	290.	254.	457.	49.
17800/4000	"	38,000	4.56	656.	3.71	534.	.088	12.7	.260	37.4	.619	89.1	High	140.	31.5	165.	297.	271.	487.	46.
3800/850	28900/6500	30,000	4.10	591.	3.35	482.	.033	4.7	.138	19.9	.094	13.5	High	21.3	4.76	17.4	31.3	.232	.418	194.
"	"	32,000	4.10	591.	3.34	481.	.032	4.6	.135	19.6	.088	12.6	High	20.	4.45	14.5	26.1	.231	.416	206.
"	"	30,000	4.11	591.	3.34	481.	.032	4.5	.133	19.1	.082	11.8	High	19.	4.16	11.9	21.5	.230	.414	219.
"	"	29,000	4.11	592.	3.34	480.7	.031	4.5	.131	18.8	.079	11.4	High	18.	4.02	10.8	19.5	.230	.414	226.

### Cage Stresses

The cage force predictions are based on average ball-pocket loading under severe ball-cage orientations. This severe orientation is unlikely except under extreme ball-speed variation<sup>[4]</sup> situations which occur under the combination of high speed and high radial loads. In this regard, under low BSV conditions a low probability is given in the force prediction. Conversely, under extreme BSV condition, a high probability of cage loading is indicated.

The predicted compressive stresses are on the order of 0.2 GPa (30,000 psi), which are probably not sufficient to induce catastrophic component failure for bearing temperatures less than about 0 C for FEP or TFE cages. However, extreme wear of the cage would be probable. In contrast, the so-called hoop stress in the cage is on the order of 0.42 GPa (60,000 psi) for the oxygen pump bearing and 0.55 GPa (80,000 psi) for the fuel pump bearing, which could cause cage breakage for cage temperatures higher than -100 C for TFE or FEP (with fabric) cages under severe BSV conditions. Therefore, under extreme radial loads, cage failure is possible.

For the oxygen pump bearings, severe cage loads are probable at bearing radial loads (total for two bearings) of 26,700 N (6000 pounds) on both the pump end and the turbine end, especially at the higher speeds. There was an anomolous point at 8900 N (2000 pounds) and 38,000 rpm where high BSV occurred. The reason for this is uncertain, but it does underscore the fact that the bearing is very marginal under these load conditions.

For the fuel pump bearing, several cage stresses probably occur at 26,700 N (6000 pounds) if a 17,800 N (4000 pounds) axial load is applied. A transient radial load of 28,900 N (6500 pounds) will cause high (but not catastrophic) cage loads if the axial load is only 3800 N (850 pounds). Here, the compressive stresses are on the order of 0.14 GPa (19,900 psi) and the hoop stresses are on the order of 0.090 GPa (13,000 psi).

### Heating Calculations

The temperature predictions in Tables 2 through 4 are the temperature rise above the cryogenic temperature. Even under severe conditions, the predicted values are only on the order of 250 C, which is probably not sufficient to damage the bearing. However, these temperatures are based on the assumption of an adequate transfer film with a friction coefficient of 0.08. If this transfer film fails under the high stresses (as is likely), the temperatures will be on the order of 2.5 times these minimum values. These temperatures could easily be above the tempering temperatures for 440C steel (315 C) and could cause a degradation in material performance. Assuming a failure of the transfer film at the ball-race interface, temperatures in excess of 315 C could occur at total radial loads in excess of 17,800 N (4000 pounds) for both the oxygen pump bearings and the fuel pump bearings, which could initiate the failure.

### Bearing Life

Serious degradation in bearing life will occur as a result of bearing overloading. However, even the pessimistic life estimates given in Tables 2-4 do not reflect possible catastrophic failure of the cage or excessive ball heating. The general conclusion is that the oxygen pump (pump end) bearing cannot realistically withstand even momentary levels of 17,800 N (4000 pounds) axial and radial loads or the order of 17,800 N (4000 pounds) radial load at high speeds (36,000 rpm or higher).

Crush Load Estimates

The axial crush load estimates for the three bearings are:

- |                          |                                                     |
|--------------------------|-----------------------------------------------------|
| 7955 (Turbine End)       | - 0.14 MN (32,000 pounds) - based on maximum stress |
|                          | - 0.48 MN (108,000 pounds) - based on mean stress   |
| 7958 (Pump End)          | - 0.12 MN (26,000 pounds) - based on maximum stress |
|                          | - 0.40 MN (89,000 pounds) - based on mean stress    |
| 7502 (Fuel Pump Bearing) | - 0.08 MN (18,000 pounds) - based on maximum stress |
|                          | - 0.27 MN (60,000 pounds) - based on mean stress.   |

Assuming a 60/40 load split, this would imply a crush load of 0.13 MN (30,000 pounds) based on maximum stress and 0.44 MN (100,000 pounds) based on mean stress.

The mean stress calculations are probably more realistic. This implies that the bearings can withstand extremely high ultimate loads before being completely destroyed. However, performance life will be lost at much lower loads as discussed in previous sections.

Calculating Units

Since the bearing drawing and all input data provided by NASA were in English units, all calculations were performed in English units. Therefore, the SI units presented in this report were converted from English units.

REFERENCES

- [1] Jones, A.B., "A General Theory for Elastically Constrained Ball and Roller Bearings Under Auxiliary Load and Speed Conditions", Trans. ASME, J. Basic Eng., Vol. 82, Ser. D., No. 2, June 1960, pp 309-320.
- [2] Kannel, J.W. and Walowit, J.A., "Simplified Analysis For Traction Between Rolling/Sliding Elastohydrodynamic Contacts", Trans. ASME, J.O.L.T., Vol. 93, Ser. F., No. 1, January 1971, pp 39-46.
- [3] Seely, F.B. and Smith, J.O., Advanced Mechanics of Materials, John Wiley and Sons, Inc., New York, 1959, pp 181, 182, and pp 342-376.
- [4] Barish, T., "Ball-Speed Variation and Its Effect on Cage Design", Lubrication Engineering, No. 25, 110, (1969).
- [5] Wyatt, O.H. and Dew-Hughes, D., Metals, Ceramics, and Polymers, Cambridge Press, Cambridge, Massachusetts, 1974, p 210.

APPENDIX A

DATA ON AISI 440C STEEL

## AISI TYPE 440C

Filing Code: SS-101  
Stainless Steel

MARCH 1960

DATA ON WORLD WIDE METALS AND ALLOYS

Published by  
Engineering Alloys Digest, Inc.  
Upper Montclair, New Jersey

### AISI TYPE 440C

(High-Carbon Chromium Stainless Steel)

AISI TYPE 440C is a hardenable high-carbon chromium steel designed to provide stainless properties with maximum hardness.

#### Composition:

Carbon	0.95-1.20
Manganese	1.25 max.
Silicon	1.00 max.
Phosphorus	0.04 max.
Sulphur	0.04 max.
Chromium	16.50-18.00
Molybdenum	0.75 max.
Iron	balance

#### Physical Constants:

Specific gravity	7.68
Density, lb./cu. in.	0.277
Specific heat, BTU/lb./°F. (32-212°F.)	0.11
Electric resistance, ohms/cir. mil. ft.	361
Thermal coef. expansion/°F. (32-212°F.)	0.0000056
* Thermal conductivity, Btu/ft <sup>2</sup> /in./hr/°F (68-212°F.)	203
Modulus of elasticity, psi	29,000,000
Structure	Martensitic

#### PROPERTIES

**Table 1—TYPICAL HEAT TREATED PROPERTIES**

(Oil quenched from 1900°F. tempered at 600°F)

Tensile strength, psi	285000
Yield strength, psi (0.2%)	275000
Elongation, % in 2"	2.0
Reduction of area, %	10.0
Brinell hardness	580
Izod impact, ft. lbs.	

**Table 2—EFFECT OF TEMPERING TEMPERATURE ON HARDNESS**

(1" Rd. oil quenched from 1900°F & tempered 1 hour)

Tempering Temperature °F.	Rockwell Hardness "C"
300	60
400	59
500	57
600	56
700	56
800	56

**Table 3—EFFECT OF TEMPERING TEMPERATURE**

(2" Rd. quenched in oil from 1900°F.)

Tempering Temperature °F.	Brinell Hardness	Rockwell Hardness "C"	Impact Strength (notched bar) ft. lbs.
As quenched	580	61.0	1.0
200	580	61.0	2.0
300	580	61.5	2.5
400	580	56.5	2.8
500	575	55.0	3.0
600	560	54.5	2.9
700	560	55.0	2.7
800	560	55.5	2.5
900	575	57.0	2.2
1000	555	52.0	2.1
1100	440	43.0	3.0

**Table 4—ANNEALED PROPERTIES**

	Process Annealed	Full Annealed
Tensile strength, psi	125000	110000
Yield strength, psi (0.2%)	100000	70000
Elongation, % in 2"	12	15
Rockwell hardness	C22 -C27	B95 - B99
Izod impact, ft. lbs.	5 - 20	5 - 20

**Table 5—MECHANICAL PROPERTIES — TEMPERED WIRE**

(0.250 inch diameter)

Tensile strength, psi	110000 - 125000
Yield strength, psi (0.2%)	65000 - 100000
Elongation, % in 2"	13 - 6
Reduction of area, %	30 - 20
Rockwell hardness	B97 - C24

**Table 6—TYPICAL MECHANICAL PROPERTIES BARS**

	Annealed	Heat Treated	Cold Drawn
Tensile strength, psi	110000	130000 - 285000	125000
Yield point, psi	65000	110000 - 275000	100000
Elongation, % in 2"	10 - 15	12 - 2	7
Reduction of area, %	30	20 - 10	20
Brinell hardness	210 - 250	275 - 600	260
Izod impact, ft. lbs.	20 - 5	8 - 3	

**Table 7—SHORT TIME TENSILE PROPERTIES**

Temperature °F.	Tensile Strength °F.
1300	30500
1700	17000
1500	16500

\*  $K = 203 \text{ BTU IN/HR FT}^2 \text{ OF} = 3.65 \text{ Ft-lb. Ft/sec Ft}^2 \text{ OF}$



**Table 8—IZOD IMPACT PROPERTIES**  
(0.394" unnotched specimens, quenched in oil from 1850°F., tempered 2 hours).

Tempering Temperature °F	Rockwell Hardness "C"	Izod Impact ft. lbs.
300	62-63	60.3
400	60-61	79.0
500	58-60	82.0
600	58-59	79.0
800	58-59	72.6
1000	57-58	51.6
1200	41-42	77.6

### Heat Treatment:

**PROCESS ANNEAL:** Heat at 1350-1450°F., cool very slowly in the furnace to 230-245 Brinell.

**FULL ANNEAL:** Heat uniformly at 1550-1600°F., soak and cool slowly in furnace to 1000-1200°F. at rate of 20-50°F. per hour, then cool in air, oil or water to 190-215 Brinell.

**HARDEN:** First preheat slowly to 1450°F. and soak, then raise temperature to 1850-1950°F., quench in warm oil or air to C55-58 Rockwell, temper immediately to desired hardness. (Do not overheat, because full hardness cannot be obtained and the steel becomes non-magnetic when overheated.) (To remove strains and yet retain maximum hardness draw at least one hour at 300-350°F.) (Air Hardening may be used for thin sections.)

Care must be taken not to overheat this steel during annealing. Any effort to produce extreme softness is dangerous and will be reflected later by poor hardening ability. Grain growth, decarburization, and the formation of a partially austenitic structure are the result of prolonged or excessive heating.

In hardening, 15 minutes at heat is sufficient to refine the structure. Maximum hardness (C-61 to C-63) is reached after oil quenching. Microstructures of pieces hardened below 1900°F. contain banded carbides, those hardened at 1900°F. contain globular carbides, and those hardened above 1925°F. show grain growth.

For a combination of maximum hardness and toughness, temper at 800°F. Avoid tempering between 800 and 1050°F., particularly if the part is subject to impact, and if hardness and other properties are to be closely controlled. Tempering from above 1100 to 1250°F. gives excellent properties, including high impact resistance, and the product is machinable when so tempered. The alloy is subject to temper brittleness when slowly cooled from this range; therefore, it should be oil quenched after tempering to give best impact strength.

### Machinability:

For most machining operations, this steel cuts best when in the dead soft annealed condition. Because of its high-carbon content it machines somewhat like high-speed steel. Chips are tough and stringy; therefore, chip curlers and breakers are important. In turning operations, reduced speeds of 40 to 60 sfpm, with feeds of 0.003 to 0.008 inch, must be used. It has a machinability rating of about 30% of AISI B1112.

### Workability:

If annealed for maximum softness, this steel can be moderately cold formed, headed and upset with slightly more difficulty than the lower carbon, lower chromium grades of stainless steel. It can be hot forged, hot headed and hot upsets. However, preheating in the range of 1400-1500°F. insures the best results in hot working. Because this steel is strongly air-hardening, all parts should be furnace cooled after hot working to prevent cracking. Warm lime or warm ashes can be used for cooling provided they are thoroughly dry.

Where forging, preheat to 1400-1500°F., then heat slowly and uniformly to 1900-2150°F. Do not forge below 1700°F. and reheat as often as necessary.

### Weldability:

Because of its high hardenability, this steel is seldom welded. However, by preheating parts to 300-400°F. before welding,

**Table 9—COMPRESSION TESTS**  
(Oil quenched from 1850°F. & tempered)

Tempering Temperature °F	Rockwell Hardness "C"	Ultimate Compressive Strength psi
As-quenched	61-61.5	445,500
300	58	391,750
400	57	378,625
600	55	338,000
1000	53	320,875
1200	35	181,000

followed by a 6 to 8 hour anneal at 1350-1400°F. and air cooling, satisfactory welds can be produced. When weld rods are required, a composition similar to the parent metal should be used.

### Corrosion Resistance:

The corrosion resistance is quite good in the hardened and tempered condition but moderate "as annealed" and consequently should only be put in service in the fully heat treated condition. Will resist such conditions as fresh water, steam, crude oil, gasoline, perspiration, alcohol, foodstuffs, etc. Maximum resistance to corrosion and tarnishing is developed only when fully hardened, and with surfaces polished to a high luster.

### Pickling Treatment:

8-12% H<sub>2</sub>SO<sub>4</sub> at 150-170°F.

6-10% HCl + H<sub>2</sub>SO<sub>4</sub> at 130-140°F.

10% HNO<sub>3</sub> + 2% HF at 120-130°F.

Pickle in the annealed or stress relieved condition to avoid pickle cracking due to relief of residual stresses.

### Specification Equivalents:

SAE 51440C

### General Characteristics:

AISI Type 440C is a general purpose hardenable stainless steel, which upon quenching develops maximum hardness together with high strength and corrosion resistance. Besides the wear resistance imparted by heat treatment, it has intrinsically superior wear resistance due to its chemical composition.

This steel is always used in the hardened condition; and after heat treatment, parts must be pickled, ground or polished to remove all scale. After pickling, parts should be baked at 250-300°F. to remove acid embrittlement. For best results, surfaces must be entirely free from foreign particles that may have been picked up in grinding or polishing. This can be done by passivating. It is not recommended for elevated temperature applications since corrosion resistance is impaired when used in the annealed condition or hardened and drawn above 800°F. It is widely used in applications where corrosion resistance, coupled with good cutting edge or abrasion resistance, are required. For best impact strength do not temper above 800°F. Do not pickle hardened material without first stress-relieving. This steel is magnetic in all conditions. Maximum operating temperature is 1500°F. for intermittent service and 1400°F. for continuous service.

### Forms Available:

Forging billets, hot rolled bars and forgings, ground bars, wire and wire rods, annealed strip.

### Application:

Pivot pins, dental and surgical instrument, cutlery, valve parts, ball bearings, nozzles, hardened steel balls and seats for oil well pumps.

### Manufacturer:

All stainless steel mills produce this type alloy under their own proprietary name or under AISI Type 440C specifications.